Temperature Dependence of Amyloid Beta-protein Fibrillization

by

YOKO HAMMOND

S. B., Massachusetts Institute of Technology
(1997)

Submitted to the Department of Physics
in partial fulfillment of the requirements for the degree of
Master of Science in Physics

at the

Massachusetts Institute of Technology

June 1999

Signature of Author: _____
Department of Physics
May, 1999

Certified by: _____
George B. Benedek
Alfred H. Caspary Professor of Physics and Biological Physics
Thesis Supervisor

Accepted by: _____
Thomas J. Greytak
Professor, Associate Department Head for Education

Temperature Dependence of Amyloid Beta-protein Fibrillization

by

Yoko Hammond

Submitted to the Department of Physics
on May 7, 1999 in partial fulfillment of the
requirements for the Degree of
Master of Science in Physics

Abstract

This thesis presents my study of Aβ fibrillogenesis in two parts. In Part 1, I review the research process that was undertaken and what I learned from it. In Part 2 of the paper I present, in the form of a reprint , the scientific finished product of this investigation which was published in PNAS and for which I am the first author. Part 2 of this thesis reports, in greater detail, the study of the temperature dependence of the Aβ fibril elongation rate constant, k_e, in 0.1 M HCl. The rate of fibril elongation was measured at Aβ monomer concentrations ranging from 50 to 400 μM and at temperatures from 4°C to 40°C. Over this temperature range, k_e increases by two orders of magnitude. The temperature dependence of k_e follows the Arrhenius law, $k_e = A\exp(-E_A / kT)$. The pre-exponential factor A and the activation energy, E_A are $\approx 6\times10^{18}$ liter/(mol·sec) and 23 kcal/mol, respectively. Such a high value of E_A suggests that significant conformational changes are associated with the binding of Aβ monomers to fibril ends.

Thesis Supervisor: George B. Benedek

Title: Alfred H. Caspary Professor of Physics and Biological Physics

To my husband

who has truly opened my eyes

Introduction

This thesis presents my study of Aβ fibrillogenesis in two parts. In Part 1, I review the research process that was undertaken and what I learned from it. In Part 2 of the paper I present, in the form of a reprint , the scientific finished product of this investigation which was published in PNAS and for which I am the first author.

In Part 1, the discussion of the research process and what I learned from it, I first present the genesis of the literature search. Next, I discuss the experimental procedure, which includes an outline of how samples were prepared and data was collected. Then, in the Data Analysis section, I discuss how the data were analyzed using constrained regularization method. In the final section of Part 1, I discuss how the results of the analysis were interpreted. In Part 2, the reprint, I present the final scientific product.

PART 1: Research Process

Literature Search

I began the research process by conducting literature review. After reading Dr. Lomakin's paper (Lomakin, A. *et.al.* (1996) *PNAS* **93,** 1125-1129), I reviewed the references and used that as the basis of a more extensive search. In addition, I gathered other information on Alzheimer's disease (AD) and its effect on the U. S. society.

The literature reports that AD is the most common cause of dementia and the fourth leading cause of death in the United States. Nearly four million people are believed to be afflicted with the disease. The costs associated with the care of those afflicted is estimated to be $136 billion in the United States alone. Current treatments only ease symptoms, providing neither a cure nor effectively retarding the progression of the disease.

Research published has identified a characteristic feature of AD patients to be the presence of amyloid plaques in their brain. Findings show that the principal constituent of amyloid plaques are amyloid β-protein (Aβ) fibrils. Pathological studies of AD brains, for example one performed by Yankner, show that neurodegenerative changes occur around compact plaques composed of Aβ fibrils (Yankner, B. A. (1996) *Neuron* **16,** 921-932). Furthermore, it has also been demonstrated that Aβ fibrils are neurotoxic *in vitro*.

Other findings suggest that Aβ fibril formation requires the presence of a nucleus. While research findings are not conclusive regarding the antecedent factors that lead to the formation of

nuclei, more conclusive finding exist regarding the growth of Aβ fibrils. For example, Naiki has found that elongation of fibrils is characteristic of first-order kinetics (Naiki, H. & Nakakuki, K. (1996) *Lab. Invest.* **74,** 374-383).

Quasielastic Light Scattering Spectroscopy (QLS) was used to monitor Aβ fibril formation. It is an optical method for quantitatively determining the diffusion coefficients of particles undergoing Brownian motion in solution (Pecora, R. (1985) *Dynamic Light Scattering*, Plenum Press, New York, NY). Sample solutions are placed in the QLS apparatus between a laser light source and a detector. Scattered light collected by the detector is a sum of scattered light from individual particles in the sample solution. The relative positions of particles within the scattering volume determine the phase difference of scattered waves from each particle. Brownian motion of the scattering particles change the phase differences for all pairs of scattered waves and as a result, the intensity of the scattered light detected becomes uncorrelated to its initial intensity. The correlation time is determined by the diffusion coefficient of scattering particles, $\tau_c \sim 1/Dq^2$, where D is the diffusion coefficient and q is the scattering vector. Thus, by measuring the temporal correlation of the fluctuating light signal, diffusion coefficients of scattering particles in the sample solution can be determined.

QLS measures the diffusion coefficient of individual scattering particles. From the diffusion coefficient, one can calculate the hydrodynamic radius of each particle using the Stokes-Einstein relation $D = k_B T/6\pi\eta R_h$, where k_B is Boltzmann's constant, T is the absolute temperature, and η is the solvent viscosity. Thus, it is advantageous to use QLS, rather than

turbidity or Fourier-transform IR spectroscopy, because it allows for the measurement of individual fibril size.

The peptide solution environment was chosen to be at pH=1. There are both advantages and disadvantages to setting the pH level to pH=1 rather than to the physiological pH. On the one hand, an advantage to setting pH=1 is that at this condition, fibril elongation rate slows down sufficiently to enable detailed monitoring of the entire fibril formation process by QLS, particularly the initial, faster elongation stage of the process. Previous QLS experiments performed at neutral pH have only been able to provide data on later stages of Aβ fibril formation. Another advantage of this condition is that it eliminates fibril-to-fibril association, a form of aggregation which makes the interpretation of QLS data more difficult. On the other hand, one of the disadvantage of performing experiments at pH=1 is that Aβ protein may take conformation different from that at physiological pH. Different conformation may lead to fibril morphology different from that found *in vivo* Another possible disadvantage is that the fibrillogenesis mechanism might operate differently at pH=1 than at physiological pH. However, as Dr. Lomakin reported (Lomakin, A. *et.al.* (1996) *PNAS* **93,** 1125-1129), Aβ fibrils formed under this condition were structurally indistinguishable from those observed in the brains of AD patients. On this basis, one may expect that the mechanisms of Aβ fibril elongation at pH=1 are the same as those operating at the physiological pH level.

Experimental Procedure

The goal of this research was to use Quasielastic Light Scattering to determine the activation energy of the binding of Aβ to the growing fibril tip and to understand the molecular

mechanism of elongation. As mentioned earlier, Aβ fibril elongation follows first-order kinetics; thus, the elongation rate k_e is described by the Arrhenius law, $k_e = A\exp(-E_A / kT)$, where E_A is the activation energy, A is the prefactor, k is Boltzmann's constant, and T is the absolute temperature. Therefore, to generate plots of k_e versus $1/T$, I used QLS to measure k_e by monitoring the rate of fibril elongation at various temperatures.

The primary procedure consisted of preparing sample of varying concentrations of Aβ solution and performing QLS measurements of the fibril elongation rate in each sample. Two sets of samples were prepared: one at high concentrations of Aβ and the other at low concentrations. High concentration samples were prepared by adding 0.1N HCl to lyophilized Aß to achieve the desired peptide concentration. Next, I vortexed the mixture for approximately 5 seconds, subsequently filtering or sedimenting large aggregates. To filter the solution, I used an Anotop 10 Plus 20 nm inorganic filter to remove large aggregates from the sample. Alternatively, I centrifuged the solution at 20,000 × g for 30 minutes to sediment aggregates. The latter procedure was adopted to reduce the amount of Aß peptide loss during the filtration process. In either case, after removing large aggregates, I aliquotted the solution into two clean test tubes to take QLS measurements.

At high concentrations (above the critical micellar concentration c^*), as Dr. Lomakin reported, Aβ monomers form micelles (Lomakin, A. *et.al.* (1996) *PNAS* **93,** 1125-1129). Nuclei, which are required for Aβ fibril elongation, form out of these micelles. At low concentrations (below c^*), however, alternative nucleation pathways predominates in the absence of Aβ micelles. Alternative nucleation, which includes, but is not limited to nucleation

on impurities, is not controllable. Therefore the sample preparation procedure outlined above proved ineffective when preparing low concentration samples. When low concentration samples were prepared in the way described above, I was unable to observe nucleation or subsequent fibril elongation; consequently, an alternative sample preparation procedure had to be developed. After exploring the issue with Dr. Lomakin, I prepared low concentration Aβ sample solutions using the following, pre-incubation method.

First, I prepared a high concentration Aβ sample solution, as in the procedure described above. Then I incubated the solution at room temperature, monitoring the fibril growth of Aβ using QLS. After about four hours, short fibrils formed from these nuclei created from micelles. I then took the solution out of the QLS apparatus and diluted it to the desired concentration. The diluted, low concentration, sample was then aliquotted into four test tubes. The samples were then divided; I took two samples for immediate QLS measurements, the others I froze at -85°C. I measured the mean diffusion coefficient of each sample over time at various temperatures. For example, in the first set of measurements, one sample was measure at 4°C and another was measured at 25°C. Once the first set of measurements were complete, the remaining two frozen samples were thawed and measured at 15°C and 35°C.

There are two QLS experimental setups available, thus I was able to make measurements of two sample solutions concurrently. For high concentration samples, I took QLS measurements at 4°C and room temperature (25°C). For lower concentration samples I took measurements at 4°C, 15°C, 25°C and 35°C. Low concentration samples, prepared by diluting high concentration ones, required less peptide and thus could be prepared in greater number. Consequently, I was able to perform a greater number of measurements at lower concentration.

Given the greater number of samples at lower concentration, I was able to gain greater resolution of the effect of temperature dependence of the elongation rate per concentration level.

During QLS measurements, I used a Coherent Innova 90 argon laser (514 nm) (Coherent, Santa Clara, CA). An argon laser was chosen because of its high signal-to-noise ratio; thus allowing me more accurately observe initial growth rates. I set the scattering angle at 90°, and controlled the temperature by using a water bath and a temperature control unit. The autocorrelator used was a 144-channel Langley Ford model 1097 (Amherst, MA).

Analysis

Once the data from QLS measurements were collected, they were analyzed in three steps. First, I used a regularization program, developed by Dr. Lomakin, and data obtained from QLS measurements to obtain temporal evolution of the mean hydrodynamic radius.

Second, I plotted the mean hydrodynamic radius vs. time. This plot showed that the rate of fibril formation was constant initially, then decreased approaching a final fibril length. I used the interpolation formula for stiff rods with diameter 8 nm to calculate the average fibril length L from R_h, as discussed later in PART 2. I then determined the total number of monomers in the fibril according to $N_f = \lambda L$, where λ is the linear density of Aβ within the fibril ($\lambda = 1.6\ \text{nm}^{-1}$). I thus determined the elongation rate $dN_f/dt = k_e c$ from the slope of the initial linear domain of the curve of R_h vs. time

Finally, I plotted the elongation rate $k_e c$ against the inverse of absolute temperature for each sample concentration. Since the elongation kinetics of Aβ fibrils is of first order, the

elongation rate obeys the Arrhenius law, $k_e = A\exp(-E_A / kT)$, where E_A is the activation energy. Thus, the slope and intercept of a line fitted to the above mentioned data yielded the activation energy E_A and the prefactor A, respectively. I calculated the activation energy to be $E_A = 23$ kcal / mol and the prefactor to be $A \approx 6\times 10^{18}$ liter / (mol · sec).

Interpretation of Data/Results

As will be discussed in PART 2, the activation entropy ΔS associated with the binding of Aβ to the growing fibril tip is can be determined. Using the transition state theory and the thermodynamic relationship $\Delta G = E_A - T\Delta S$, the activation entropy can be related to the prefactor A as $\Delta S = R\ln(A/\upsilon^{1/3} D)$. Using the values for the prefactor and the activation energy obtained, I calculated the entropy associated with the activation process and the free energy of the activation to be $T\Delta S = 16$ kcal/mol (at 300 K) and $\Delta G = 7$ kcal / mol, respectively.

While discussing with Dr. Lomakin the results of our analysis and how they might be interpreted, it was hypothesized that a significant conformational change, such as protein unfolding, may be associated with the activation process of Aβ fibril elongation. This hypothesis led me to conduct an additional literature review on protein folding. Based on the results from this review of the literature, it seems reasonable to assume that protein unfolding is a possible mechanism of the conformational change. The complete discussion is found in the reprint of the paper attached in the next section.

Through this research process, I learned several experimental methods, such as QLS, HPLC, and EM, that are particularly useful in studying proteins. I also learned how scientific

research is conducted, from identifying a problem and developing a strategy to presenting results in a form of a manuscript and subsequently identifying a new problem based on the results obtained. Most importantly, it has trained me to approach a problem with a critical mind. I believe that this research project has greatly helped me develop as a scientist.

PART 2: Reprint of *PNAS* (1998) **95,** 12277-12282.

Temperature Dependence of amyloid β-protein fibrillization

Yoko Kusumoto, Aleksey Lomakin, David B. Teplow, and George B. Benedek

Dept. of Physics and Center for Materials Science and Engineering, MIT, Cambridge, MA 02139

Center for Neurologic Diseases, Brigham and Women's Hospital, Boston, MA 02115

Introduction

Alzheimer's disease (AD) is the most common cause of dementia and the fourth leading cause of death in the United States[1]. AD is characterized by the deposition of the 40 to 42-residue amyloid β-protein (Aβ) in the cerebral parenchyma and vasculature and by the formation of intracellular neurofibrillary tangles[2]. Two major types of deposit are distinguished, on the basis of the presence or absence of fibrillar Aβ aggregates[2].Those deposits containing fibrillar elements are associated with areas of damaged neuropil, whereas afibrillar deposits are found within otherwise normal tissue[3]. *In vitro*, fibrillar forms of Aβ are toxic to neuronal cells[3,4]. The deposition of fibrillar Aβ is thus thought to be a seminal event in the pathogenesis of AD[5]. An increasing body of genetic evidence supports this conclusion[6]. In particular, mutations that increase the overall production of Aβ, that increase the relative amount of the particularly

amyloidogenic 42-residue form of the peptide, or that facilitate Aβ deposition have been found to cause familial forms of AD.

The central role of fibrillar Aβ in AD pathogenesis suggests that therapeutic approaches focused on the fibrillogenesis process would be highly promising. Detailed knowledge of the mechanism of Aβ fibrillogenesis helps to identify specific steps in the fibrillogenesis process to which a drug might be targeted. This knowledge, together with information on the production of Aβ monomers and the kinetics of Aβ fibril degradation, is also needed to foresee the consequences of intervention at a particular stage of fibrillogenesis. These considerations have stimulated active investigations of the kinetics of Aβ fibrillization.

In vitro studies have suggested that Aβ fibrillogenesis occurs in two distinct stages, nucleation and elongation of fibers[7]. The nucleation stage is a series of thermodynamically unfavorable steps leading to the creation of a stable nucleus. It is not clear at present how big the nucleus is. The smallest particles detected in the fibrillogenesis process at low pH have sizes that correspond to the diameter of an Aβ fibril[8]. This finding is consistent with the view that nuclei are very short fibrils. Heterogeneous nucleation, e.g., on non-Aβ seeds, may also occur, which is a plausible mechanism for the nucleation of Aβ fibrils *in vivo*. *In vitro*, preexisting heterogeneous nuclei or Aβ seeds present a serious experimental problem. The length that fibrils reach when all soluble peptide is exhausted is inversely proportional to the total number of nucleated or preexisting fibrils. In turn, the length of the fibrils is the key parameter that determines the kinetics of fibril-to-fibril aggregation, or sedimentation of fibril aggregates, or gelation of the solution. Thus, lack of control of the number of seeds leads to poor

reproducibility, both in fibrillogenesis kinetics and in the macroscopic properties of the aggregated Aβ sample.

Elongation of an individual fibril, however, is a well defined process that is insensitive to variation in nucleus or seed concentration. There is significant experimental evidence that the kinetics of the elongation process is of the first order, i.e., Aβ monomers bind to fibril ends with a rate proportional to their concentration c[8,9,10]:

$$\frac{dN_f}{dt} = k_e c \,. \qquad \textbf{(1)}$$

Here, N_f is the number of monomers in a fibril. The proportionality coefficient relating the elongation rate dN_f/dt to the concentration of Aβ monomers is termed the elongation rate constant, k_e. For the sake of simplicity, the term "monomer" is used to describe the soluble form of Aβ that adds to fibril ends. It has been assumed in the past that soluble, nonfibrillar Aβ was monomeric; however, the possibility exists that soluble Aβ is actually dimeric[11,12].

The elongation rate constant is a fundamental characteristic of the fibrillogenesis process. It varies with solution conditions such as pH, ionic strength, and temperature and can be altered by chemical reagents capable of binding to the Aβ monomer itself or to a fibril end. Quantitative determination of the effects of fibrillogenesis conditions on k_e provides valuable leads to understanding the molecular mechanism of fibril elongation.

Several methods have been used to study the kinetics of Aβ fibrillogenesis. The simplest method, turbidimetry, monitors the total light scattering from the sample[13,14]. The intensity of scattered light grows proportionally to the molecular weight of the scattering particles and ideally

would reflect fibril elongation. In practice, however, the bulk of the scattering intensity arises from fibril-to-fibril association. The kinetics of fibril association depends on fibril size, concentration, and whether the sample is stirred. These factors make quantitative interpretation of turbidimetry results extremely difficult, if not impossible.

Naiki *et al.*[9] have used thioflavine T binding to study the kinetics of Aβ fibril elongation. This method measures the total concentration of fibrillar Aβ, which increases at the rate $k_e cN$, where N is number concentration of fibrils. Because N is unknown, it is impossible to determine the value of k_e. However, by comparing samples of identical concentration, seeded with the same number of fibrils, Naiki *et al.* were able to study relative temperature and pH dependencies of k_e [9], as well as the effect of apolipoprotein E on the elongation rate[15].

Quasielastic light scattering (QLS), in contrast, allows the simultaneous, noninvasive monitoring of both size and molecular weight of particles in solution and is particularly well suited for studying protein aggregation phenomena[16]. This method has been used successfully to study the late stages of fibrillogenesis and the effect of sample preparation procedures on the fibrillization process[17,18]. The principal difficulty in using QLS is the same as for the less sophisticated turbidimetry method: fibril-to-fibril association can lead to the formation of large aggregates, which dominate the light scattering and complicate data interpretation. In our previous study[8], we discovered that fibrillization of Aβ in 0.1 M HCl is highly reproducible, is free from fibril-to-fibril association, and yields fibrils that are morphologically indistinguishable from those formed *in vivo*. QLS was used to monitor both nucleation and elongation of Aβ fibrils and to determine quantitatively the elongation and nucleation rate constants. These studies

lead to development of a full mathematical description of the fibrillogenesis process.[19] In this publication, we present our study of the temperature dependence of the elongation rate of Aβ fibrils in 0.1 M HCl and report the activation energy required for the binding of Aβ monomers to fibril ends.

Materials and Methods

Protein Preparation. Peptide synthesis, purification, and characterization have been described previously[8,11]. Briefly, Aβ(1-40) was made on an automated peptide synthesizer (Applied Biosystems model 430A) using 9-fluorenylmethoxycarbonyl-based methods. Reverse-phase high-performance liquid chromatography was used for peptide purification. Quantitative amino acid analysis and matrix-assisted laser desorption/ionization time-of-flight mass spectrometry yielded the expected composition and molecular weight. The purified peptide was stored as a lyophilizate at -20°C.

Experimental Protocol. We first conducted experiments to establish that the temperature dependence of elongation rates follows the Arrhenius law. Aβ was dissolved in 0.1 M HCl (pH=1) at 4°C to a nominal concentration of 250 μM, vortexed gently, and filtered through a 20-nm inorganic membrane filter (Anotop 10 Plus, Whatman) into a QLS cuvette. The sample was then incubated for 4 hr at 25°C. As reported previously[8], at this concentration, Aβ monomers form micelle-like structures that serve as centers of nucleation. The sample was monitored by QLS, and, after 4 hr, when fibrils were ≈ 120 nm long (hydrodynamic radius $R_h \approx 20\,\text{nm}$), was diluted 5-fold and aliquotted equally among four new cuvettes. One cuvette was used for

monitoring fibrillogenesis at the highest temperature (35°C), while the other three were frozen and kept at -85°C. Preliminary experiments showed no detectable alteration in the course of fibrillogenesis in samples that had been frozen and thawed. After the fibrillization process in the first sample was complete, each of the remaining aliquots was thawed sequentially and the time dependence of fibril size was monitored at 25°C, 15°C, and 4°C. This procedure ensured identical numbers of fibrils as well as identical total Aβ concentration in each aliquot. However, before the incubation at each temperature, there was already considerable elongation of fibrils. Such significant growth diminished the accuracy with which the value of the elongation rate could be measured. To improve this accuracy, we performed a series of experiments in which samples were monitored at different temperatures immediately upon dissolution. Lyophilized peptide was dissolved and filtered as above, then split into halves. The fibrillogenesis in the aliquots was then monitored concurrently in two separate spectrometers held at two different temperatures, typically 4°C and 25°C. Such concurrent measurements of fibrillogenesis at two different temperatures were performed at nominal concentrations of 100, 125, 250, and 375 μM. The 125 μM sample was centrifuged at 20,000 × g for 30 min rather than being filtered.

In each experiment, when fibrillogenesis was complete, the total Aβ concentration was determined by amino acid analysis. These final concentrations were less, sometimes significantly less, than the nominal concentration that was calculated from the weight of the initially dissolved material. Part of the loss was likely because of removal of preexistent fibrils and aggregates during filtration. As will become clear in the next section, the uncertainty in the initial concentration of soluble Aβ is insignificant for the estimation of the thermodynamic parameters of the binding reaction between Aβ monomer and fibril end.

QLS and Data Analysis. QLS measurements were performed with a 144-channel Langley Ford model 1097 correlator (Amherst, MA) and a Coherent Innova 90 argon laser (514 nm) (Coherent, Santa Clara, CA). The scattering angle was 90°. The temperature was controlled by using an Endocal bath (Neslab Instruments, Portsmouth, NH) and a temperature control unit with a feedback loop for fine-tuning.

A constrained regularization method was used to determine the mean diffusion coefficient, $\overline{D}$ [20]. The mean hydrodynamic radius R_h was calculated using the Stokes-Einstein relation $\overline{D} = k_B T/6\pi\eta R_h$, where k_B is Boltzmann's constant, T is the absolute temperature, and η is the solvent viscosity. The average fibril length L was then calculated from R_h, assuming that fibrils are stiff rods with diameter 8 nm, using an interpolation formula[8]. Finally, the total number of monomers in the fibril was determined according to $N_f = \lambda L$, where λ is the linear density of Aβ within the fibril ($\lambda = 1.6\ \mathrm{nm}^{-1}$)[17]. By monitoring $\overline{D}$, the temporal evolution of $R_h(t)$ or $N_f(t)$ may thus be determined. The elongation rate $dN_f/dt = k_e c$ was determined from the slope of the initial linear domain of the curve of R_h vs. time.

Results and Discussion

We formulated previously a theoretical description of Aβ fibrillogenesis at low pH[19]. We established that Aβ monomers form micelle-like structures above a critical concentration, $c^* \approx 100\ \mu\mathrm{M}$[8]. Nuclei arise from these micelles, and fibrils grow from nuclei through the addition of Aβ monomers to the fibril ends. This fibrillogenesis mechanism is supported by the

data presented in Figure 1. This figure shows the time evolution of the size distribution of the scattering particles in a 250 μM Aβ solution. Immediately on dissolution, the major contribution to the light scattering comes from particles with hydrodynamic radii of ≈ 7 nm (Figure 1*A*). These particles are never observed at Aβ concentrations below c^*. This fact, together with the known amphiphilic potential of Aβ monomer[21] and a theoretical analysis of the kinetics of Aβ fibrillogenesis[8], is consistent with the 7-nm peak in Figure 1 representing micelle-like aggregates of Aβ monomers. Over time, a new peak emerges (Figure 1*B-F*). The average R_h for this peak is bigger than that of the micelles and increases with time. The intensity of the scattered light also increases and is nearly proportional to the size of the scattering particles (data not shown). The proportionality between average size and intensity of scattering is indicative of one-dimensional (fibrillar) growth of the scattering objects. We therefore ascribe this distribution to mature Aβ fibrils. Indeed, electron microscopy and circular dichroism experiments performed on equivalent samples reveal fibrils with quaternary and secondary structures indistinguishable from those observed in fibrils from plaques[8].

After 4 hr of incubation, when fibrils reached $R_h \approx 20\,\text{nm}$, a sample was diluted to 50 μM, divided into four aliquots, and further fibril growth was monitored at 4°C, 15°C, 25°C, and 35°C. We found that the elongation rates vary dramatically with temperature. Figure 2 displays on a logarithmic scale the initial elongation rates dN_f/dt as a function of inverse temperature. These data points could be fit well with a straight line. According to Equation 1, the elongation rate is $k_e c$, where the concentration of monomers c is a temperature-independent quantity. Therefore, the elongation rate constant follows the Arrhenius law:

$$k_e = A\exp\left(-E_A/RT\right). \qquad \textbf{(2)}$$

The slope of the straight line in Figure 2 determines the activation energy E_A, which was calculated to be 22.8 ± 1.1 kcal/mol (1 kcal = 4.18 kJ). Measurements represented in this figure were performed on the preincubated samples with identical starting concentrations of Aβ and identical starting number concentrations of fibrils. Moreover, after dilution, the only process that occurs in these samples is the elongation of fibrils, with the rate dependent on the temperature. Thus, the curves for the time evolution of the apparent hydrodynamic radius differ only in the scale of time which is set by k_e. However, a more accurate determination of the elongation rate constant requires measurements of the size evolution of shorter fibrils at the initial stage of the fibrillogenesis process, since for shorter fibrils the relative increase in the fibril length is much more pronounced. Also, entanglement of longer fibrils modifies their diffusion. This leads to a systematic overestimation of the length of the fibrils as determined from QLS data. At the same mass concentration of fibrils, this type of error is much less significant for short fibrils than for long ones.

In Figure 3, we show the temporal evolution of the mean hydrodynamic radius of Aβ fibrils incubated at two different temperatures immediately upon dissolution. The nominal concentration of Aβ was 250 μM and the measurements were taken at 24°C (+) and 4°C (O). We see from the initial slopes of the curves that the elongation rate increased dramatically with temperature. By using the interpolation formula relating the average hydrodynamic radius R_h to fibril length L [8], the elongation rates were calculated to be 18.6 nm/hr for 24°C and 1.0 nm/hr for 4°C. An increase in the temperature by 20°C results in an increase in the elongation rate by a

factor of 20. Although the two samples used for these measurements came from the same initial solution, it was possible that identical numbers of fibrils would not be nucleated in each, because these two samples were kept at different temperatures and the nucleation rate could be temperature-dependent. However, as seen in Figure 3, the final size of fibrils was similar at both temperatures. Because the total concentration of peptide was the same, this indicates that approximately equal numbers of fibrils were, in fact, nucleated in each sample. The activation energy determined from these measurements yielded the same value as the less accurate procedure using controlled nucleation (Figure 2). Clearly, our measurement of the elongation rate is insensitive to the nucleation step of the fibrillogenesis process. This is expected because the QLS method measures the length of individual fibrils. The results of such measurements are insensitive to variations in the number concentration of fibrils, assuming noninteracting particles.

In Figure 4, we summarize all our data in a semilogarythmic plot of the initial elongation rates of Aβ fibrils. The dashed line is a linear fit to the 50 μM sample data from Figure 2. Measurements carried out concurrently at two different temperatures for Aβ samples of concentration 100 μM (Δ, ∇), 125 μM (◊), 250 μM (✧), and 375 μM (□) all yielded approximately the same value for the activation energy, $E_A = 23.0 \pm 0.6$ kcal/mol. This coincided, within the statistical error, with the value found for the samples with controlled nucleation. Note that the last three nominal concentrations are above c^*. At concentrations of soluble Aβ above the critical concentration, the concentration of free monomers is effectively fixed at c^* and the elongation rate should therefore be $k_e c^*$[8,19]. The identical slopes of the Arrhenius plots determined above and below c^* indicate that this critical micellar concentration

is independent of the temperature, within our experimental error. Taking $c^* = 100$ μM, the value of the preexponential factor A in Equation 2 is $\approx 6 \times 10^{18}$ liter/(mol·sec).

We may analyze the above results in the framework of transition state theory for the rate of chemical reaction between free Aβ monomer and fibril end[22]. We assume that the monomer can bind to the fibril tip only when it is inside the reaction volume υ with the characteristic size $l \approx \upsilon^{1/3}$. We also assume that the monomers entering the reaction volume can actually bind to a fibril only if these monomers or the fibril tip (or both) are in the appropriate activation state. The probability of the occurrence of such a state is $\exp(-\Delta G / kT)$, where ΔG is the change in free energy associated with the activation process. Thus the rate of fibrillar growth can be written as

$$\frac{dN_f}{dt} = \Gamma \exp\left(-\Delta G/RT\right) \qquad \textbf{(3)}$$

where Γ is the number of monomers entering the reaction volume per unit time. To estimate Γ, we note that the rate with which monomers enter a certain volume is equal to the rate with which they leave this same volume. The average number of monomers in a volume υ at any moment of time is $c\upsilon$. These monomers are in a constant Brownian motion and diffuse out of this volume in a time $\tau \approx l^2 / D \approx \upsilon^{2/3} / D$, to be replaced by others. Thus the number of monomers entering the reaction volume per unit time is $c\upsilon / \tau$, and therefore

$$\Gamma \cong c\upsilon^{1/3} D. \qquad \textbf{(4)}$$

It is reasonable to assume that the size of the reaction volume is of the order of the size of a monomer. Note that in this case the magnitude of the "encounter time" τ becomes comparable to the characteristic time constant for the monomer reorientation, i.e., to the reciprocal of the

monomer rotational diffusion coefficient. Implicit in our derivation of Equation 3 is the assumption that the "encounter time" τ that the monomer spends within the reaction volume is short compared to the lifetime τ_A of an activated state. If this were not the case, the possibility of activation during the encounter would need to be taken into account. We shall justify the assumption $\tau << \tau_A$ later.

Substituting Equation 4 into Equation 3, using the thermodynamic relationship $\Delta G = E_A - T\Delta S$, where ΔS is the change in the entropy associated with the activation process, and comparing with Equation 1, we have

$$k_e = \upsilon^{1/3} D \exp(\Delta S / R) \exp\left(-E_A / RT\right). \qquad \textbf{(5)}$$

Equation 5 permits a physicochemical interpretation of the significance of the parameters A and E_A, as obtained from the experimental measurements of $k_e(T)$ (Equation 2). One can see from comparison of Equation 5 and Equation 2 that the activation entropy ΔS is related to the parameter A by

$$\Delta S = R \ln\left(\frac{A}{\upsilon^{1/3} D}\right). \qquad \textbf{(6)}$$

In this equation, the diffusion coefficient of the free monomer, D, is 1.6×10^{-7} $\mathrm{cm}^2 \cdot \mathrm{sec}$ (for $R_h = 1.8\,\mathrm{nm}$).[11] Because of the uncertainty in the initial concentration of free Aβ monomers and the value of c^*, the quantity $A \approx 6 \times 10^{18}$ $\mathrm{liter}/(\mathrm{mol} \cdot \mathrm{sec})$ is known only within a factor of 2. The reaction volume size $l = \upsilon^{1/3}$ is also not well known. We may take it to be of the order of the dimension of the Aβ monomer, namely ≈ 1 nm. Using these values in Equation 6 provides $\Delta S = 5.3 \times 10^{-2}$ $\mathrm{kcal}/(\mathrm{K} \cdot \mathrm{mol})$ or $T\Delta S = 16$ kcal/mol at 300 K. Although the values used to

calculate the activation entropy are not known accurately, even a factor of 10 uncertainty in the magnitude of $A/\upsilon^{1/3}$ introduces an error of only $2.3RT = 1.4$ kcal/mol in $T\Delta S$, which is less than 10% of the total value of ≈ 16 kcal/mol. Note that, in comparison with the uncertainty in $\upsilon^{1/3}$, the error in the numerical value of A caused by a poorly known monomer concentration c produces an insignificant effect on the deduced value of the activation entropy ΔS.

The change in free energy associated with the activation process, $\Delta G = E_A - T\Delta S = 7$ kcal/mol, is a relatively small quantity, so the probability of an activated state occurring, $\exp(-\Delta G/RT) \approx 10^{-5}$, is sufficiently large for the reaction to occur at the observed rate. However, this small free energy results from the difference between the much larger activation energy $E_A = 23.0$ kcal/mol and the entropy contribution, $T\Delta S = 16$ kcal/mol (at 300 K). The activated and inactive states differ significantly in both energy and entropy, suggesting a substantial difference in structure. Several factors may contribute to the increased entropy of the activated state, including unfolding of protein and release of bound water molecules. Since activation is also accompanied by a significant increase in energy, it is likely that a transition from a more ordered, bound structure to a more disordered, loose structure is the essence of the activation process preceding monomer binding to a growing fibril.

It is illuminating to compare the thermodynamics of Aβ activation with that of conformational change of peptides of similar size. In Table 1, we present the values of E_A, $T\Delta S$, and ΔG, as determined in the present paper for Aβ, and those for the unfolding (melting) of several peptides with known secondary structures. These include chymotrypsin inhibitor 2[23], the N-terminal domain ($\lambda_{6\text{-}85}$) of phase λ repressor[24,25], the SH3 domain of spectrin[26], and the C-

terminal fragment (41-56) from protein GB1[27]. Table 1 shows that the thermodynamic parameters of Aβ activation are of the magnitude expected for conformational rearrangement of a peptide of this size. A key question is where this rearrangement occurs, i.e., in the soluble monomer, at the fibril tip, or in both. Recent studies[28] indicate that soluble Aβ monomer may not possess a stable structure which could "unfold" in the activation process. On the other hand, amyloid fibrils do have a stable structural organization[5]. It is therefore conceptually attractive to envision a partial unfolding of the organized fibril end to accommodate addition of an incoming Aβ monomer. This process would involve bond breaking among Aβ monomers constituting the fibril tip with its obligatory activation energy, partial unfolding of these molecules with a resultant increase in entropy, and subsequent bond reformation and entropic loss concurrent with incorporation of the new, incoming Aβ molecule.

We now examine numerically the validity of our assumption that $\tau << \tau_A$. Using the values of D and l established above, we estimate the encounter time $\tau = l^2 / D \approx 70$ ns. We expect this time to be small compared to the "lifetime" of the activated "unfolded" state. [Note that the lifetime of the inactive state is $\exp(\Delta G / RT) \approx 10^5$ longer than the activated one.] For comparison, the time constant associated with the kinetics of β-hairpin formation for the GB1 protein fragment[27] listed in Table 1 is 3.7 μsec. This time is more than an order of magnitude larger than the estimated encounter time between an Aβ monomer and a fibril tip. The GB1 protein fragment is small compared to Aβ and even more so compared to the fibril tip. For larger peptides, the kinetics of folding slows down dramatically. For instance, the time constant for $\lambda_{6\text{-}85}$ folding is about 300 μsec[24]. These comparisons justify our assumption that the encounter

between Aβ monomer and fibril tip is so short that the possibility of transitions between active and inactive conformations during this moment can be ignored.

A significant conformational change is required for a binding reaction to occur. The probability of this change, $\exp(\Delta G / RT)$, is a key factor in determining the Aβ fibril elongation rate constant k_e. A natural deduction from this fact is that chemical interventions that stabilize the inactive state of soluble Aβ monomer or fibril tip can have a very profound effect on the rate of Aβ fibrillogenesis. To increase ΔG, these interventions should either lower the energy of the inactive state of Aβ or decrease the entropy of the activated, unfolded state, or both. One can also envision strategies targeting the growing fibril tip. A simple example is competitive inhibition by a ligand that can block fibril elongation by binding to the fibril tip. If the equilibrium dissociation constant K is very small, even a moderate concentration of the ligand, C_L, will "poison" the growing tip of the fibril and reduce the elongation rate by the factor K/C_L. This factor is simply the probability that the fibril tip is free of a ligand molecule, provided $C_L >> K$. Within the framework of our analysis, the effect of such a ligand can be described as an increase in the activation free energy ΔG by the quantity $RT\ln(C_L / K)$, which is essentially the free energy needed to remove the ligand from the fibril tip.

Conclusions

Using QLS spectroscopy, we studied the fibrillogenesis of Aβ(1-40) in 0.1 M HCl solution and measured, as a function of temperature, the rate constant k_e for Aβ fibril elongation. Within the temperature range 4-40°C, we have found that the elongation rate varies

over two orders of magnitude and obeys the Arrhenius law. The activation energy of the reaction, $E_A = 23.0$ kcal/mol, indicates that Aβ monomer binding to fibril tip proceeds via an activated state. Accordingly, we have used transition state theory for reaction kinetics to estimate the entropy change associated with the transition into the activated state. This theory assumes that the lifetime of the activated state is much longer than the encounter time between monomer and fibril tip. We have estimated that the activation process involves a very significant increase in entropy, $T\Delta S = 16$ kcal/mol at 300 K. These values for E_A and $T\Delta S$ are consistent with the notion that the activation process involves unfolding of Aβ within the growing fibril tip, of soluble Aβ, or both.

The magnitude of the dependence of the elongation rate constant on the free energy of activation clearly indicates that the activation step in binding of monomer to fibril end is a prime target for therapeutic inhibitors of fibril growth. Indeed, agents that increase the energy required for activation or decrease the entropy in the activated state should produce a profound reduction in the elongation rate. The present findings indicate that theoretical analysis of measurements of the magnitude and temperature dependence of fibril elongation rates can provide valuable insights into the process of monomer addition at the growing fibril tip. Furthermore, our results demonstrate that experimental methodology based on the QLS method can serve as a powerful quantitative assay to test the efficacy of putative inhibitors of Aβ fibril growth.

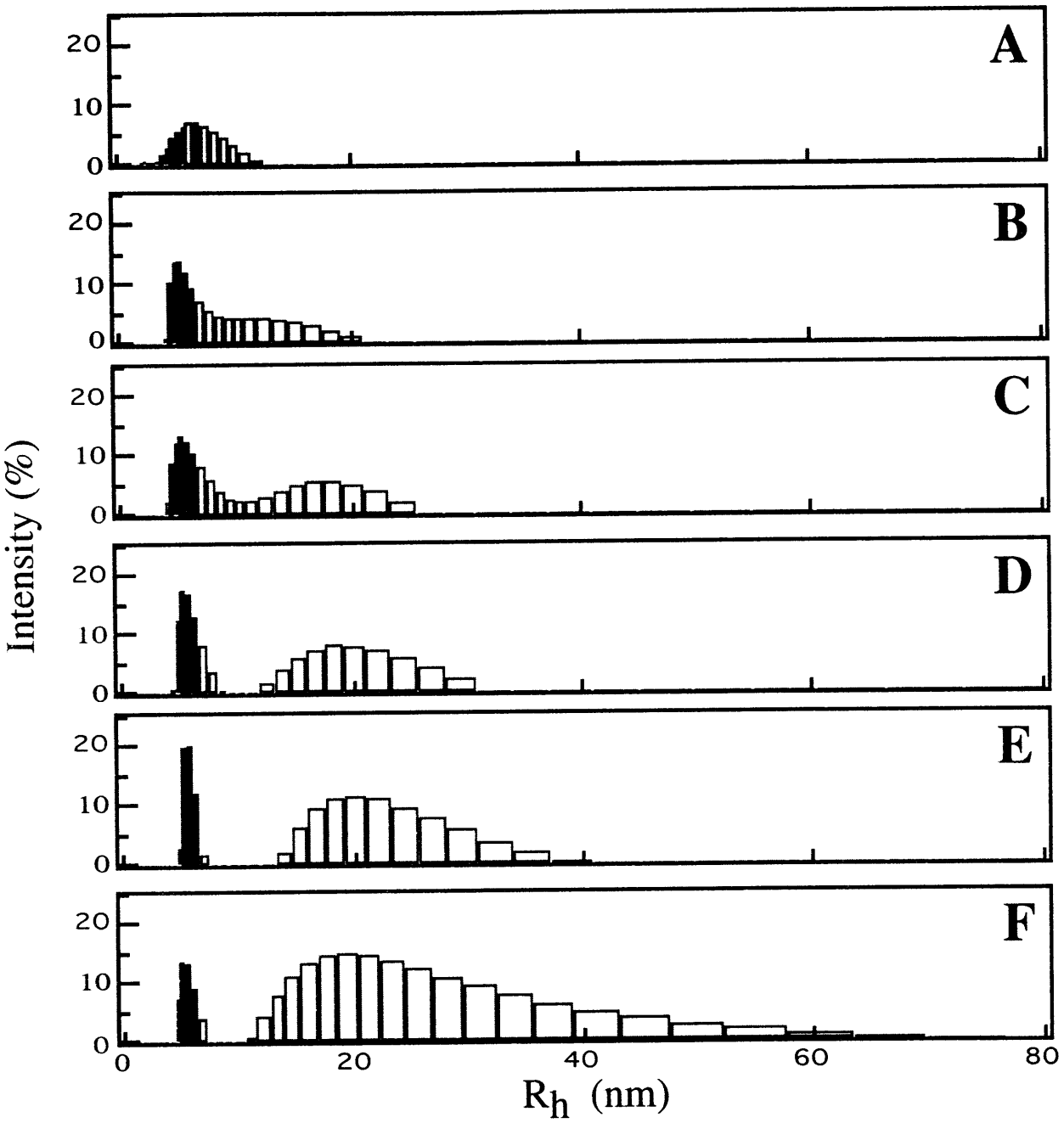

Figure 1 Temporal evolution of the size distribution of the scattering particles in a 250 μM Aβ solution. (A) One hour after sample preparation. The major contribution to scattering comes from micelle-like aggregates of Aβ monomers with $R_h \approx 7$ nm. (B-F) Distribution of scattering particles at 1.5 hr (B), 2 hr (C), 3 hr (D), 4 hr (E), and 6 hr (F) after sample preparation. A second distribution, with an average R_h larger than 7 nm, emerges from the micellar distribution and grows in size over time. This second distribution is produced by mature Aβ fibrils.

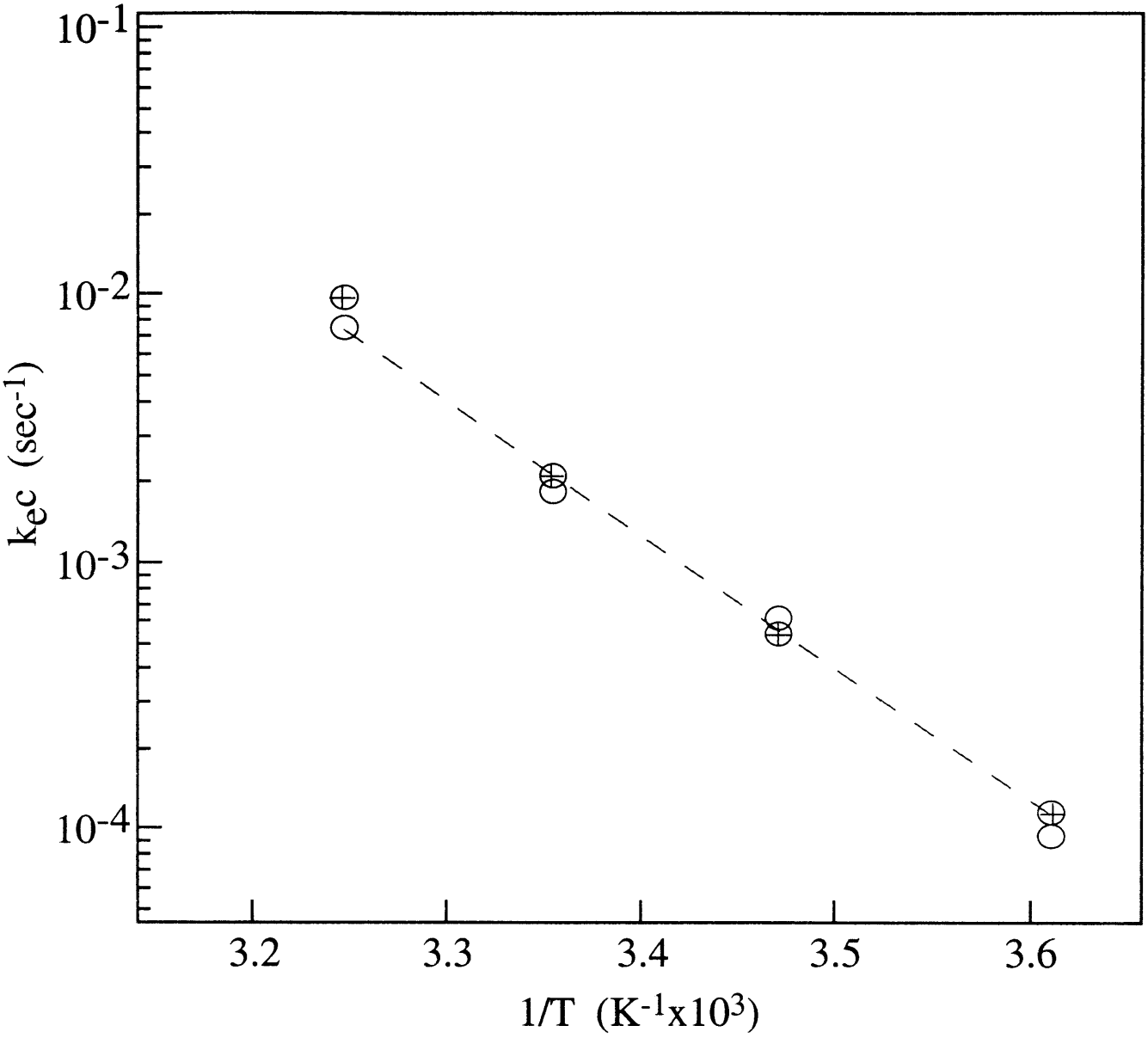

Figure 2 Arrhenius plot of initial elongation rate vs. inverse temperature for 50 μM samples. Two sets of samples (O,⊕) were prepared under controlled nucleation conditions. The resulting data could be fit well with a straight line ($R = -0.99$), whose slope yielded an activation energy, E_A, of 22.8 ± 1.1 kcal / mol.

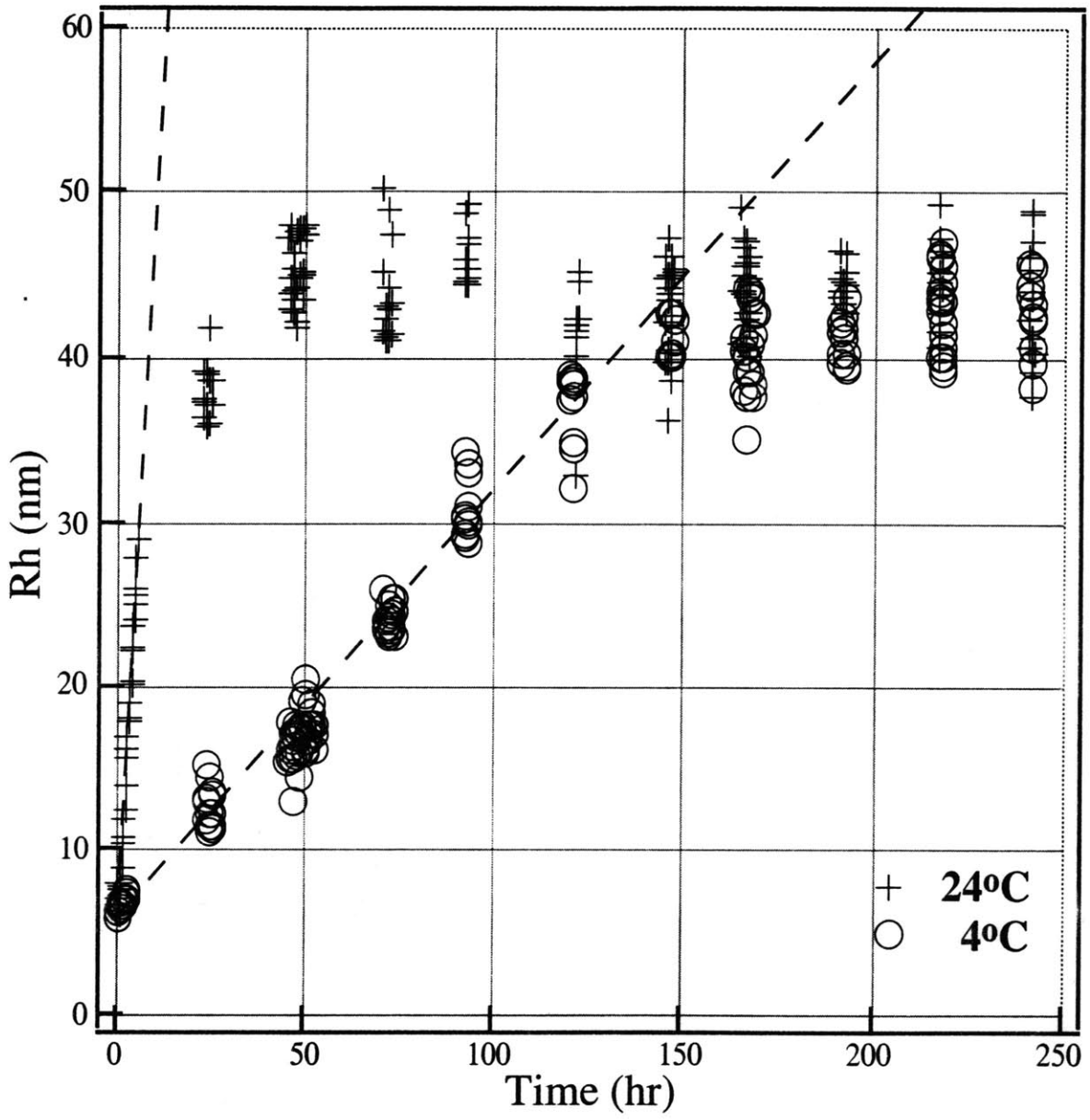

Figure 3 Temporal evolution of the mean hydrodynamic radius R_h of Aβ fibrils. Samples of Aβ at 250 μM concentration were incubated at 24°C (+) and 4°C (O). Slopes of dashed lines indicate initial elongation rates at each temperature.

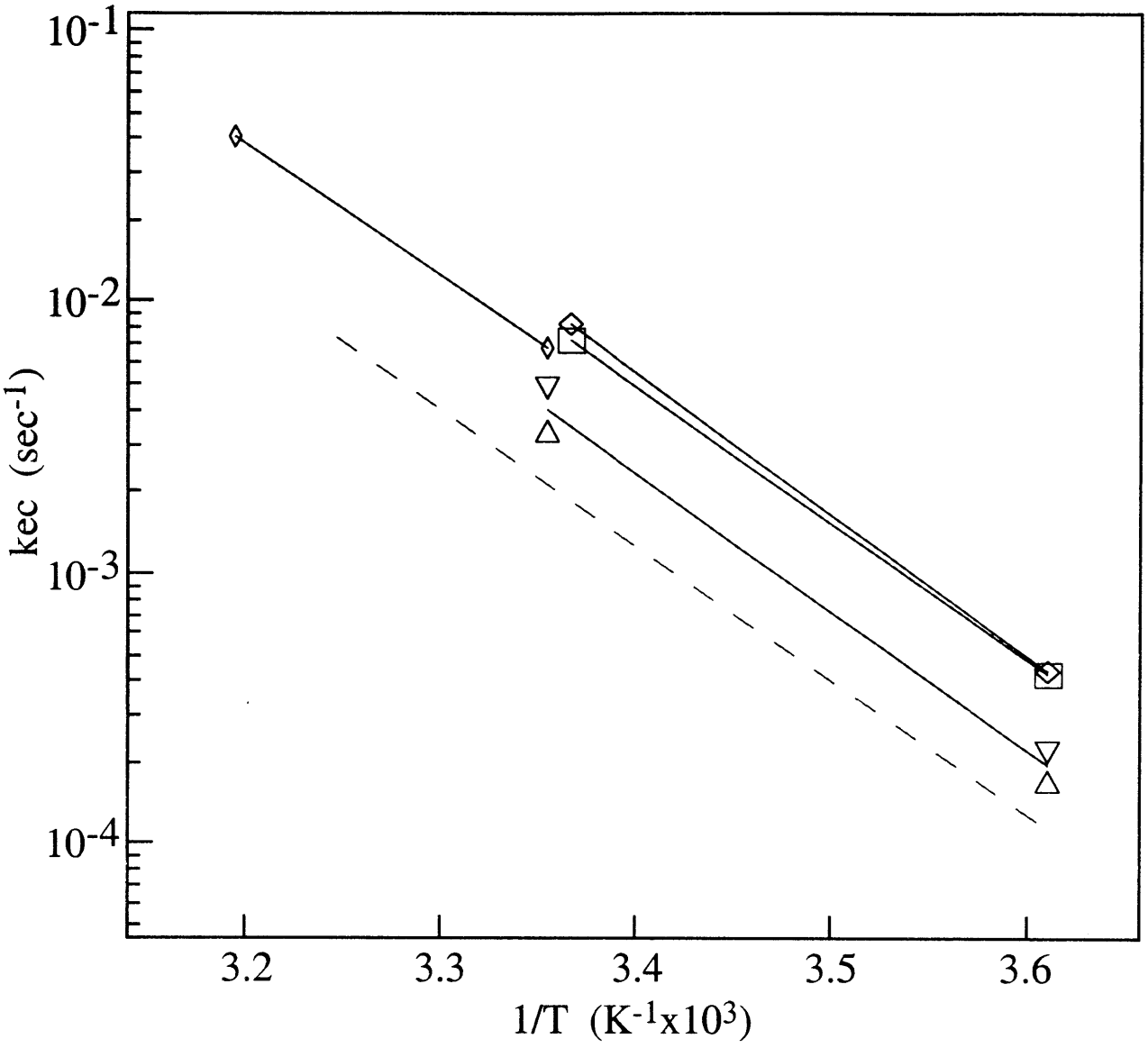

Figure 4 Arrhenius plot of elongation rates as a function of inverse temperature. Nominal Aβ concentrations are 100 μM (Δ, ∇), 125 μM (◊), 250 μM (✧), and 375 μM (□). The dashed line is the linear fit of the data for the 50 μM samples presented in Figure 3. Samples with nominal concentrations of 125 and 100 μM, which are only slightly above c^*, actually showed elongation rates of approximately 0.8 and 0.4, respectively, of the maximal value $k_e c^*$. Clearly, in the process of preparation, the concentrations of soluble Aβ were reduced in the 25 μM sample to $0.8\,c^*$ (centrifugation) and in the 100 μM sample to $0.4\,c^*$ (filtration). Furthermore, the estimated concentration of free monomers in the preincubated sample immediately after dilution was 25 μM (Figure 3; O,⊕). This value is consistent with the fact that fibrils of about half the expected final length were formed, suggesting that aproximately half of the initial 250 μM concentration of free monomers was consumed before the 5-fold dilution of the sample.

Table 1 Thermodynamic parameters for small peptides.

Peptides	No. of residues	E_A (ΔH)	$T\Delta S$	ΔG	Structure
Aβ	40	23.0±0.6	≈16	≈7	?
CI2[26]	64	31.2	24.6	6.5	α
λ repressor[27, 28]	80	16.1±0.1	12.8	3.3	α/β
SH3[29]	62	9.5	6.5	3.0	β
GB1(41-56)[30]	16	11.6	11.7	0.1	β-hairpin

E_A, $T\Delta S$, and $\Delta G = E_A - T\Delta S$ are in kcal/mol. $T = 300\,\mathrm{K}$ for all peptides except for λ repressor, which was studied at 37°C (310 K).

[1] Iqbal, K. (1991) in *Alzheimer's Disease: Basic Mechanisms, Diagnosis, and Therapeutic Strategies,* eds. Iqbal, K., McLachlan, D. R. C., Winblad, B. & Winsniewski, H. M. (Wiley, New York), pp. 1-5.
[2] Selkoe, D. J. (1991) *Neuron* **6,** 487-498.
[3] Yankner, B. A. (1996) *Neuron* **16,** 921-932.
[4] Selkoe, D. J. (1996) *J. Biol. Chem.* **271,** 18295-18298.
[5] Selkoe, D. J. (1994) *J. Neuropathol. Exp. Neurol.* **53,** 438-447.
[6] Hardy, J. (1997) *Trends Neurosci.* **20,** 154-159.
[7] Jarrett, J. T. & Lansbury, P. T. Jr., (1993) *Cell* **73,** 1055-1058.
[8] Lomakin, A., Chung, D. S., Benedek, G. B., Kirschner, D. A. & Teplow, D. B. (1996) *Proc. Natl. Acad. Sci. USA* **93,** 1125-1129.
[9] Naiki, H. & Nakakuki, K. (1996) *Lab. Invest.* **74,** 374-383.
[10] Esler, W. P., Stimson, E. R., Ghilardi, J. R., Vinters, H. V., Lee, J. P., Mantyh, P. W. & Maggio, J. E. (1996) *Biochemistry* **35,** 749-757.
[11] Walsh, D. M., Lomakin, A., Benedek, G. B. & Teplow, D. B. (1997) *J. Biol. Chem.* **272,** 22364-22372.
[12] Garzon-Rodriguez, W., Sepulveda-Becerra, M., Milton, S. & Glabe, C. G. (1997) *J. Biol. Chem.* **272,** 21037-21044.
[13] Andreu, J. M. & Timasheff, S. N. (1986) *Methods Enzymol.* **130,** 47-59.
[14] Jarrett, J. T., Berger, E. P. & Lansbury, P. T., Jr. (1993) *Biochemistry* **32,** 4693-4697.
[15] Naiki, H., Gejyo, F. & Nakakuki, K. (1997) *Biochemistry* **36,** 6243-6250.
[16] Cohen, R. J. & Benedek, G. B. (1975) *Immunochemistry* **12,** 349-351.
[17] Tomski, S. J. & Murphy, R. M. (1992) *Arch. Biochem. Biophys.* **294,** 630-638.
[18] Shen, C. L. & Murphy, R. M. (1995) *Biophys. J.* **69,** 640-651.
[19] Lomakin, A., Teplow, D. B., Kirschner, D. A. & Benedek, G. B. (1997) *Proc. Natl. Acad. Sci. USA* **94,** 7942-7947.
[20] Braginskaya, T. G., Dobitchin, P. D., Ivanova, M. A., Klyubin, V. V., Lomakin, A. V., Noskin, V. A., Shmelev, G. E. & Tolpina, S. P. (1983) *Phys. Scr.* **28,** 73-79.
[21] Soreghan, B., Kosmoski, J. & Glabe, C. (1994) *J. Biol. Chem.* **269,** 28551-28554.
[22] Eisenberg, D. & Crothers, D. (1979) *Physical Chemistry* (Benjamin/Cummings, Menlo Park, CA), pp. 242-244.
[23] Jackson, S. E. & Fersht, A. R. (1991) *Biochemistry* **30,** 10428-10435.
[24] Huang, G. S. & Oas, T. G. (1995) *Proc. Natl. Acad. Sci. USA* **92,** 6878-6882.
[25] Scalley, M. L., Yi, Q., Gu, H., McCormack, A., Yates, J. R., III & Baker, D. (1997) *Biochemistry* **36,** 3373-3382.
[26] Viguera, A. R., Martinez, J. C., Filimonov, V. V., Mateo, P. L. & Serrano, L. (1994) *Biochemistry* **33,** 2142-2150.
[27] Muñoz, V., Thompson, P. A., Hofrichter, J. & Eaton, W. A. (1997) *Nature (London)* **390,** 196-199.
[28] Teplow, D. B. (1998) *Amyloid* **5,** 121-142.